

Integrated Process Design and Control of Multi-element Reactive Distillation Processes

Seyed Soheil Mansouri^a, Mauricio Sales-Cruz^b, Jakob Kjøbsted Huusom^a, Rafiqul Gani^a

^aDepartment of Chemical and Biochemical Engineering, Technical University of Denmark, Lyngby, Denmark

^bDepartamento de Procesos y Tecnología, Universidad Autónoma Metropolitana-Cuajimalpa, Ciudad de México, Mexico

(E-mails: seso@kt.dtu.dk, asales@correo.cua.uam.mx, jkh@kt.dtu.dk, rag@kt.dtu.dk)

Abstract: In this work, integrated process design and control of reactive distillation processes involving multi-elements is presented. The reactive distillation column is designed using methods and tools which are similar in concept to non-reactive distillation design methods, such as driving force approach. The methods employed in this work are based on equivalent element concept. This concept facilitates the representation of a multi-element reactive system as equivalent binary light and heavy key elements. First, the reactive distillation column is designed at the maximum driving force where through steady-state analysis it is shown that it has the least energy consumption and carbon footprint. Next, through analytical and dynamic analysis it is verified that the control structure, disturbance rejection and the controllability at the maximum driving force is the best compared to any other design alternative which does not operate at the maximum driving force.

© 2016, IFAC (International Federation of Automatic Control) Hosting by Elsevier Ltd. All rights reserved.

Keywords: Reactive distillation, Process design, Process Control, Multi-element system, Driving force

1. INTRODUCTION

As a common practice, process design and process control problems are considered as independent problems; and therefore, solved sequentially. To this end, a sequential approach is being considered where the process design is performed with respect to steady-state economic objectives, followed by controller design considering dynamic constraints and control objectives. However, as it is well-known, this sequential approach has its drawbacks as it does not address the trade-offs between conflicting design and control objectives for the chemical processes. For example, infeasible operating points, process overdesign or under-performance. Therefore, a robust performance may not always be guaranteed (Ricardez-Sandoval *et al.*, 2009). To avoid these drawbacks, several alternatives, to address process design and controllability issues simultaneously, in the early stages of process design have been proposed (Hamid *et al.*, 2010). This simultaneous synthesis approach provides optimal/near optimal operation and more efficient control of chemical processes. Most importantly, it is possible to identify and eliminate potentially promising design alternatives that may have controllability problems.

Reactive distillation column (RDC) is a multifunctional unit operation, which incorporates separation and reaction in a single operation, attracting considerable interest in research from academia and industry. Reactive distillation provides more sustainability, safer environmental performance as well as better energy management (Mansouri *et al.*, 2013). However, as a result of integration of functions/operations into one system the controllability region of reactive distillation processes is smaller due to the loss in degrees of

freedom and the process becomes non-linear with highly interacting dynamics.

Jantharasuk *et al.* (2011), proposed a new design methodology for reactive distillation processes involving multi-element systems which employs the traditional graphical tools similar in concept to design of non-reactive distillation columns, such as McCabe-Thiele method and driving force approach of Bek-Pedersen and Gani (2004). Moreover, Mansouri *et al.* (2015) proposed, integrated process design and control of binary element reactive distillation processes. In this work, their approach is extended using the design methodology by Jantharasuk *et al.* (2011) for the integrated process design and control of multi-element reactive distillation processes and the criteria of selecting the optimal design and the controller structure selection will be presented. In order to demonstrate the application of this approach, production of methyl-tert-butyl-ether (MTBE) from methanol and isobutene with 1-Butene as an inert compound is considered (a quaternary compound reactive system).

2. REACTIVE DISTILLATION COLUMN DESIGN

In this work, the well-known production of MTBE by reactive distillation from isobutene (*i*-Butene) and methanol (MeOH) with 1-Butene as an inert compound is selected to highlight the integrated process design and control of multi-element reactive distillation processes. The MTBE reaction is exothermic and reversible. It takes place in presence of an acidic catalyst, such as sulfuric acid, acidic ion-exchange resins, or other acidic catalysts. The advantages of reactive distillation have been well established in the case of MTBE.

The RDC design targets and feed specifications for production of MTBE are summarized in Table 1. The feed is considered to be introduced to the column at 11 atm and 320K. The pressure drop across the column is assumed to be negligible. Note, this is a conceptual demonstrative example and the design targets are obtained from Pérez-Cisneros (1997).

Table 1. Design targets and product specifications

Component	Structure	Feed	Distillate	Bottom
<i>i</i> -Butene	C ₄ H ₈	0.590	0.773	0.061
Methanol	CH ₄ O	0.343	0.000	0.012
1-Butene	C ₄ H ₈	0.067	0.196	0.024
MTBE	C ₅ H ₁₂ O	0	0.031	0.907

The design-control multi-objective optimization function is given as follows:

$$f_{obj} = \min \left(w_1 P_1 + w_2 P_2 + w_3 \frac{1}{P_3} \right) \quad (1)$$

In equation (1), P_1 represents costs associated to the reboiler and condenser duties. P_2 is the sensitivity of the controlled variables to disturbances in the feed (dy/dd). P_3 is the sensitivity of manipulated variables u with respect to controlled variables y (dy/du). Note that in equation (1), w_1 , w_2 and w_3 are weight factors.

2.1. Reactive distillation column design – Multi-element system

The element-based approach was first defined by Michelsen (1995) in order to calculate the element composition in vapour and liquid phases as the solution to chemical-physical equilibrium problem. The simultaneous solution to the chemical and physical equilibrium is important to predict the limits of conversion and separation in particular for a reaction-separation process such as reactive distillation systems. The problem is solved as the simultaneous solution of (2) and (3).

$$\min G(n) = \sum_{\beta=1}^{NP} \sum_{i=1}^{NC} n_i^\beta \mu_i^\beta \quad (2)$$

$$\sum_{\beta=1}^{NP} \sum_{i=1}^{NC} A_{j,i} n_i^\beta - b_j = 0 \quad (3)$$

In (2) and (3), n_i is the molar amount of component i , μ_i is the chemical potential of component i , NP is number of phases, NC is the number of components, β is the phase of concerning system, and $A_{j,i}$ is the number of times the reaction invariant element j has appeared in molecule i .

Using the Gibbs free energy minimisation approach, the solution procedures by which the multicomponent chemical and physical equilibrium is expressed as an “element phase” equilibrium problem were proposed Pérez-Cisneros et al. (1997). One of the main features of this method is its ability to handle the problem of reaction-phase equilibrium in the same manner as the case when no reactions are taking place in the system. The implementation of the element concept can be described by considering the fact that the molecules and atoms are invariant in course of a reaction. In the case of

MTBE synthesis, isobutene and methanol (two reactants) with molecular structures C₄H₈ and CH₄O, it is always true that the MTBE (product) must contain the molecular structure of isobutene and methanol (C₅H₁₂O). Since inert compound (1-butene) is also present in the reaction system, the element specification should be provided independently for that component. Therefore, the number of elements is related to the number of components as well as the reactions given there are no stoichiometric constraints in the reaction; and it is given as follows:

$$M = NC - NR \quad (4)$$

In this case, there are four components and one reaction; therefore the system can be represented as a multi-element system of three elements with the element matrix given in Table 2.

Table 2. The element matrix for MTBE synthesis.

Element	Component			
	<i>i</i> -Butene (1)	MeOH (2)	MTBE (3)	1-Butene (4)
A	1	0	1	0
B	0	1	1	0
C	0	0	0	1

In order to design the RDC involving a multi-element system, the selection of key elements is necessary. That is, the key elements are the two elements in the multi-element system that the separation is based on their specifications. Therefore, a light key element (LK) is the one that is more volatile than non-key elements and the heavy key element (HK) is the one that is less volatile than non-key elements. Therefore, the rest of the elements are grouped as non-key elements. In this context, light non-key elements (LNKs) are the ones that have a higher volatility than the LK; and the ones that are less volatile than HK are termed as heavy non-key elements (HNKs). Therefore, this representation is similar in concept to the method of distillation design for a non-reactive multicomponent system proposed by Hengstebeck (1961). Note that LK and HK are selected according to the rules of key element selection given by Jantharasuk *et al.* (2011). It is well-known that the sum of mole fractions is always equal to 1. Therefore, it is also the case when the mole fractions are given in terms of elements. Thus, the sum of mole fractions in a multi-element system is as follows:

$$W_{LK}^\beta + W_{HK}^\beta + W_{LNK}^\beta + W_{HNK}^\beta = 1 \quad (5)$$

Having the above summation, now one can represent the above multi-element system in a new composition domain termed as “equivalent binary element composition” as follows (Jantharasuk *et al.*, 2011):

$$W_{eq}^\beta = W_{LK}^\beta + W_{HK}^\beta = 1 - \sum (W_{LNK}^\beta + W_{HNK}^\beta) \quad (6)$$

where, the light key equivalent element composition is given as follows:

$$W_{LK,eq}^\beta = \frac{W_{LK}^\beta}{W_{LK}^\beta + W_{HK}^\beta} \quad (7)$$

and the element composition is given as below:

$$W_j^\beta = \frac{\sum_{i=1}^{NC} A_{j,i} x_i^\beta}{\sum_{i=1}^{NC} \sum_{j=1}^M A_{j,i} x_i^\beta} \quad (8)$$

Having the equivalent binary element concept introduced, similar methods that are used for designing binary non-reactive distillation processes, such as driving force approach and McCabe-Thiele method, can be used to design a RDC involving a multi-element reactive system. Note that in order to use the aforementioned methods, vapour-liquid equilibrium (VLE) data is required. This data is either obtained through their availability or computation of reactive bubble points or dew points. In this work, the reactive bubble point algorithm by Pérez-Cisneros (1997) is employed to calculate the VLE data for entire composition domain. In order to obtain the reactive data-set, Wilson thermodynamic model for prediction of the liquid phase behaviour and SRK equation of state for prediction of vapour phase behaviour were used. It must be noted that the calculation of reactive VLE data set is in terms of compounds. Therefore, a quaternary compound data set is obtained. Next, this data set is converted into a ternary element data set using (8). At this point, it is important to select the key elements according to the rules of key element selection. The key elements are identified as element A as the LK and element B as the HK. Therefore, now using (7), the light key equivalent element composition in vapour and liquid phase is calculated. Fig. 1 shows the temperature (T)- $W_{LK,eq}^v - W_{LK,eq}^l$ diagram for MTBE reactive system containing multi-elements.

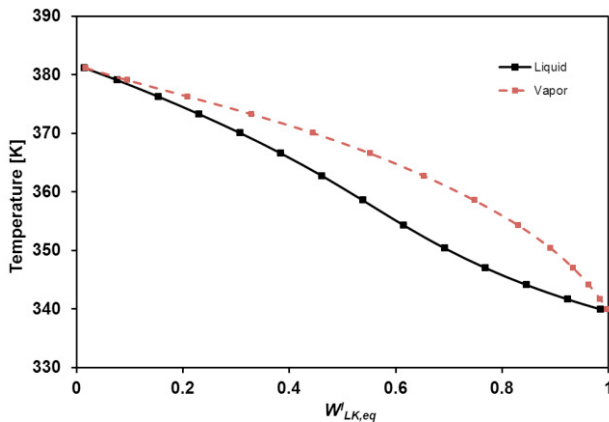


Fig. 1. $T - W_{LK,eq}^v - W_{LK,eq}^l$ diagram for MTBE reactive system ($P = 11$ atm).

The design task is to fulfil the product target specifications (see Table 1) given the feed conditions. Therefore, the important reactive distillation design variables, that are number of stages, reflux and/or reboil ratio, and the feed location need to be identified in such way that the design targets are fulfilled. To this end, the driving force method of Bek-Pedersen and Gani (2004) is employed.

The driving force approach has been originally developed to design the binary non-reactive distillation columns to operate at the maximum of driving force. This means that at the maximum location of driving force diagram, the largest possible area is utilized. Similar in concept to non-reactive

systems, the equivalent binary element driving force is defined as the difference in composition between two coexisting phases, which in case of multi-element systems they are defined by equivalent element composition. Moreover, the driving-force diagram can only exploit binary interaction between compounds, elements or equivalent elements in two co-existing phases, or two compounds on a solvent-free basis. Note that the binary equivalent based reactive driving-force diagram fully considers the extent of reaction on an equivalent element basis, and it is applied in the design of multi-element reactive distillation columns. The driving force diagram based on binary equivalent elements is defined as (Jantharasuk et al., 2011):

$$DF_{LK,eq} = W_{LK,eq}^v - W_{LK,eq}^l = \frac{W_{LK,eq}^l \alpha_{LK,eq}}{1 + W_{LK,eq}^l (\alpha_{LK,eq} - 1)} - W_{LK,eq}^l \quad (9)$$

Where,

$$\alpha_{LK,eq} = \frac{W_{LK,eq}^v / W_{LK,eq}^l}{W_{HK,eq}^v / W_{HK,eq}^l} = \frac{K_{LK}}{K_{HK}} \quad (10)$$

This is a visual and simple approach which provides the foundation to determine the important reactive distillation design variables. Fig. 2 depicts the equivalent binary element driving force diagram for MTBE multi-element reactive system at 11 atm. Moving away from the maximum driving force towards lower values, the separation becomes more difficult and as it approaches zero it becomes infeasible. On the other hand, moving toward the maximum driving force, the separation becomes easier due to the larger difference between vapour and liquid phase compositions. Therefore, from a process design point of view, the separation process must be designed/selected at the highest possible value of driving force which as a natural consequence results in optimal design with respect to energy consumption (Bek-Pedersen and Gani (2004)).

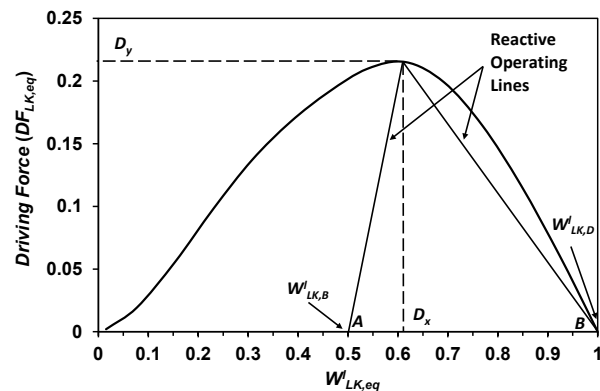


Fig. 2. Equivalent binary element driving force diagram for MTBE multi-element reactive system.

As it can be seen in the Fig. 2, the area of operation based on light key equivalent binary element composition is identified on the x -axis of the equivalent binary element driving force diagram which is feed, distillate and bottom light key equivalent composition (i.e. 0.5 and 1 for the distillate and bottom compositions based on the equivalent LK element). The lines AD_y and BD_y are drawn and their corresponding

slope is determined (see Fig. 2). The slopes of these lines correspond to minimum reboil ratio (RB_{min}) and minimum reflux ratio (RR_{min}), respectively. Next the real reflux ratio (RR) and reboil ratio (RB) are determined from $RR = 1.2(RR_{min})$ and $RB = 1.2(RB_{min})$. Note however, in this case, the number of stages for the RDC is not given. In order to obtain the minimum number of theoretical stages to perform the separation task reactive equilibrium curve based on light key equivalent element is constructed and the number of stages is obtained using McCabe-Thiele method. Fig. 3 shows the results of application of McCabe-Thiele method to find the minimum number of theoretical stages for MTBE multi-element reactive system.

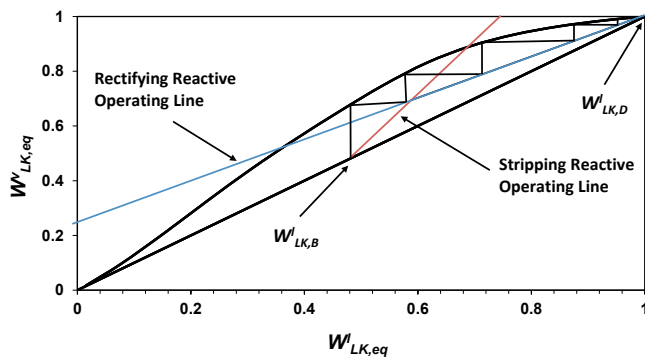


Fig. 3. Finding the minimum number of theoretical stages using McCabe-Thiele method for the MTBE multi-element reactive system

As it can be readily observed in Fig. 3, the RDC has five reactive stages. Note that from a practical point of view, presence of reaction in reboiler and condenser is infeasible and has not been reported in the literature to the best of authors' knowledge. Therefore, two non-reactive stages (i.e. partial reboiler and total condenser) are considered as stages. Thus, the total number of stages including reboiler and condenser is seven. Here, the optimal feed location is identified using driving force. Therefore, the optimal feed location can be determined by (11) as follows:

$$N_F = N(1 - D_x) \quad (11)$$

In (11), N is the number of stages which was found to be 7 according to the McCabe-Thiele method and D_x is the value corresponding to the maximum driving force on the x -axis. The optimal feed location is identified to be stage 4 from the top of the column considering the additional rules given by Bek-Pedersen and Gani (2004).

2.2. Steady-state analysis

In order to verify that the design using equivalent element driving force approach has fulfilled the design targets, steady-state simulation has been performed. Furthermore, to verify that the design at the maximum driving force is also the optimal in terms of energy consumption, an alternative feasible design which is not operating at the maximum driving force is selected for comparison. The design details for the optimal RDC design at the maximum driving force and the alternative design are summarized in Table 3.

Table 3. Design specifications for the optimal and alternative reactive distillation designs.

Design variable	Optimal	Alternative
Number of Stages (N)	7	7
Feed Stage (N_F)	4	2
Boilup ratio	1.27	3.90
Reflux ratio	2.83	7

The steady-state simulation was performed and it was verified that both designs given in Table 2 fulfil the design targets. Fig. 4, presents the comparison between the reboiler and condenser duties for the above mentioned designs together with their corresponding carbon footprint (LCSoft (Kalakul et al., 2014) was used to calculate the carbon footprint). It can be readily observed that the design at the maximum driving force has a lower energy consumption and the carbon footprint is at its lowest without any additional effort. However, in this work only carbon footprint incurred by operating conditions is considered. Further investigation is required to determine the carbon footprint contribution by equipment through their corresponding life cycle. Note however, the carbon footprint is directly proportional to energy demand of the process and it is always minimal/near minimal at the maximum driving force.

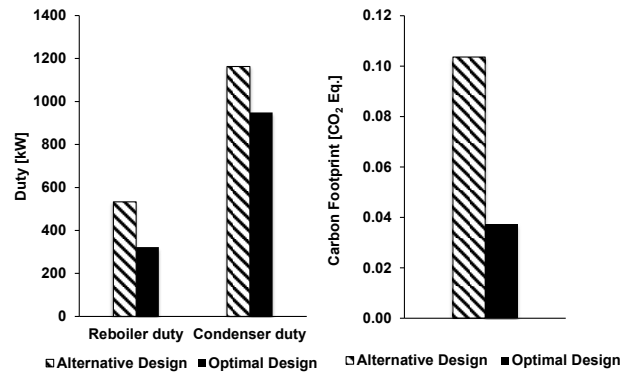


Fig. 4. Steady-state analysis of the design optimal design and an alternative design not at the maximum driving force

3. OPTIMAL DESIGN-CONTROL SOLUTION

From a process design point of view, a set of process design objectives (specifications) are determined at the maximum equivalent element driving force that satisfy for specified inputs, u , and disturbances, d , values for states, x , and outputs, y . Here, x and y also represent some of the operational conditions for the process. From a controller design point of view, for any changes in d and/or set point values in y , values of u that recovers the process to its optimal designed condition at the maximum equivalent element driving force are determined. Note that the solution for x and y is directly influenced by θ (the constitutive variables such as reaction rate or equilibrium constant). This concept is illustrated through representation of a dynamic process system in Fig. 5. The optimal solution for x (states) and y (outputs) can be obtained at the maximum point of the equivalent element driving force; see diagram in Fig. 2 which is based on θ (the constitutive variables). By using model analysis, the corresponding derivative information with

respect to x , y , u , d and θ are obtained (to satisfy controller design objectives).

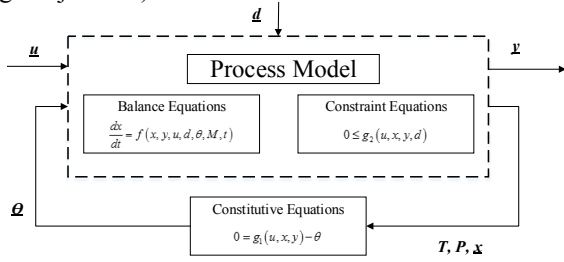


Fig. 5. Dynamic process system representation

As it was shown in section 2, selecting the design targets at the maximum driving force for designing the RDC, the optimal design objectives are obtained. Furthermore, at these design targets, from a controller point of view, the controllability and operability of the process is best achieved. This means that, the value of the derivative of controlled variables y with respect to disturbances in the feed, d , dy/dd and manipulated variables, u , dy/du will determine the process sensitivity and influence the controller structure selection. Accordingly, dy/dd and dy/du are defined as (Russel et al., 2002):

$$\frac{dy}{dd} = \left(\frac{dy}{d\theta} \right) \left(\frac{d\theta}{dx} \right) \left(\frac{dx}{dd} \right) \quad (12)$$

$$\frac{dy}{du} = \left(\frac{dy}{d\theta} \right) \left(\frac{d\theta}{dx} \right) \left(\frac{dx}{du} \right) \quad (13)$$

The values for $d\theta/dx$ can be obtained from the process (dynamic and/or steady state) constraints:

$$\frac{dx}{dt} = f(x, y, u, d, \theta, Y, t) \quad (14)$$

and values for $dy/d\theta$, dx/dd and dx/du can be obtained from constitutive (thermodynamic) constraints:

$$0 = g(u, x, y) - \theta \quad (15)$$

3.1. Selection of controlled variables

The primary controlled variable is the x -axis value on the driving force diagram which is $W_{LK,eq}^1$ (see Fig. 2). This resembles the element composition of the light key equivalent element. The secondary controlled variables are the product composition (design targets), which are measurable variables and they are at the top and bottom of the column, $W_{LK,eq}^d$ and $W_{LK,eq}^B$ (based on equivalent elements). The reason behind this selection is that conceptual variables (that is driving force, DF) cannot be measured directly.

3.2. Sensitivity of controlled variables to disturbances

In order to calculate the sensitivity, apply a chain rule to relate the derivatives of primary controlled variable to the derivatives of the secondary controlled variables. In order to apply the chain rule where the design variables vector is $y =$

$[W_{LK,eq}^d \ W_{LK,eq}^B]$, $x = DF$, is selected on the y -axis of the driving force diagram. The disturbance vector is, $d = [F_f \ z_{W_f}]$ (feed flowrate and feed composition of light equivalent element). Therefore, the chain rule is expressed as in equation (16) using equation (12):

$$\frac{dy}{dd} = \begin{bmatrix} \frac{dW_{LK,eq}^d}{dF_f} & \frac{dW_{LK,eq}^d}{dz_{W_f}} \\ \frac{dW_{LK,eq}^B}{dF_f} & \frac{dW_{LK,eq}^B}{dz_{W_f}} \end{bmatrix} = \begin{bmatrix} \left(\frac{dW_{LK,eq}^d}{dDF_{LK,eq}} \right) \left(\frac{dDF_{LK,eq}}{dF_f} \right) \left(\frac{dW_{LK,eq}^1}{dF_f} \right) & \left(\frac{dW_{LK,eq}^d}{dDF_{LK,eq}} \right) \left(\frac{dDF_{LK,eq}}{dF_f} \right) \left(\frac{dW_{LK,eq}^1}{dz_{W_f}} \right) \\ \left(\frac{dW_{LK,eq}^B}{dDF_{LK,eq}} \right) \left(\frac{dDF_{LK,eq}}{dF_f} \right) \left(\frac{dW_{LK,eq}^1}{dF_f} \right) & \left(\frac{dW_{LK,eq}^B}{dDF_{LK,eq}} \right) \left(\frac{dDF_{LK,eq}}{dF_f} \right) \left(\frac{dW_{LK,eq}^1}{dz_{W_f}} \right) \end{bmatrix} \quad (16)$$

Since the driving force diagram is always concave, therefore, the value of $dDF_{LK,eq}/dW_{LK,eq}^1 = 0$ at the maximum driving force.

Therefore, the least sensitivity of controlled variables to disturbances is achieved at the maximum driving force and (17) is obtained as follows:

$$\frac{dy}{dd} = \begin{bmatrix} \frac{dW_{LK,eq}^d}{dF_f} & \frac{dW_{LK,eq}^d}{dz_{W_f}} \\ \frac{dW_{LK,eq}^B}{dF_f} & \frac{dW_{LK,eq}^B}{dz_{W_f}} \end{bmatrix} \approx \begin{bmatrix} 0 & 0 \\ 0 & 0 \end{bmatrix} \quad (17)$$

3.3. Selection of the controller structure

The potential manipulated variables are, $u = [L \ V]$, which are represented by reflux ratio (RR) and reboil ratio (RB). Hence, the sensitivity of the secondary controlled variables to the manipulated variables is calculated after some mathematical derivation similar to those by Mansouri et al. (2015), except the fact that here the derivations are based on equivalent binary elements instead of binary elements. Interested reader can refer to the above mentioned paper to obtain detailed analytical solution. Thus, (18) presents the sensitivity of controlled variables, y , to manipulated variables, u , as follows:

$$\frac{dy}{du} = \begin{bmatrix} \frac{dW_{LK,eq}^d}{dRR} \\ \frac{dW_{LK,eq}^d}{dRB} \\ \frac{dW_{LK,eq}^B}{dRR} \\ \frac{dW_{LK,eq}^B}{dRB} \end{bmatrix} = \begin{bmatrix} DF_{LK,eq} + (RR+1) \left(\frac{dDF_{LK,eq}}{dW_{LK,eq}^1} \right) \left(\frac{dW_{LK,eq}^1}{dRR} \right) + \frac{dW_{LK,eq}^1}{dRR} \\ (RR+1) \left(\frac{dDF_{LK,eq}}{dW_{LK,eq}^1} \right) \left(\frac{dW_{LK,eq}^1}{dRB} \right) + \frac{dW_{LK,eq}^1}{dRB} \\ \frac{dW_{LK,eq}^1}{dRR} - \left(\frac{dDF_{LK,eq}}{dW_{LK,eq}^1} \right) \left(\frac{dW_{LK,eq}^1}{dRR} \right) RB \\ \frac{dW_{LK,eq}^1}{dRB} - DF_{LK,eq} \end{bmatrix} \quad (18)$$

Assuming that $dW_A^1/dRR = dW_A^1/dRB = 0$, (19) is obtained (this corresponds to a system with no or little cross interactions between y and u since changes in u cannot propagate through column). The best controller structure is easily determined by looking at the value of dy/du . It is noted from (19) that since the values of dW_A^1/dRR and dW_A^1/dRB are bigger, controlling $W_{LK,eq}^d$ by manipulating RR and controlling $W_{LK,eq}^B$ by manipulating RB will require less control action.

Therefore, for the optimal design obtained at the maximum driving force, the control structure is always given by equation (19) and it is verified by analytical analysis that it is the optimal-design control structure.

$$\frac{dy}{du} = \begin{bmatrix} \frac{dW_{LK,eq}^d}{dRR} & \frac{dW_{LK,eq}^d}{dRB} \\ \frac{dW_{LK,eq}^B}{dRR} & \frac{dW_{LK,eq}^B}{dRB} \end{bmatrix} = \begin{bmatrix} DF_{LK,eq} & 0 \\ 0 & -DF_{LK,eq} \end{bmatrix} \quad (19)$$

3.4. Rigorous closed-loop simulation

In order to verify that the best controllability is achieved at the maximum driving force, the controller structure given by (19) is implemented on the designs given in Table 2 (i.e. optimal design and an alternative one) using a proportional-integral (PI) controller. The controller parameters were tuned using IMC rules (Rivera *et al.*, 1986). The performance metrics that are used to characterize the performance of the controllers are the integral of the absolute error (IAE) and the total variation (TV) of inputs, defined by (20) and (21) as well as controller cost.

$$IAE = \int_0^{\infty} |y - y_{sp}| dt \quad (20)$$

$$TV = \sum_{i=1}^{\infty} |u_{i+1} - u_i| \quad (21)$$

Fig. 6 and Fig. 7 show the closed-loop performance of the MTBE multi-element reactive distillation process operating at the maximum driving force (optimal design), and the alternative design, not at the maximum driving force (see Table 2) in the presence of a disturbance in the feed. The disturbance scenario is a +16.5% step change in the methanol flowrate in the feed after 3.4 hrs which also corresponds to a change in feed composition since a single feed RDC is considered in this work.

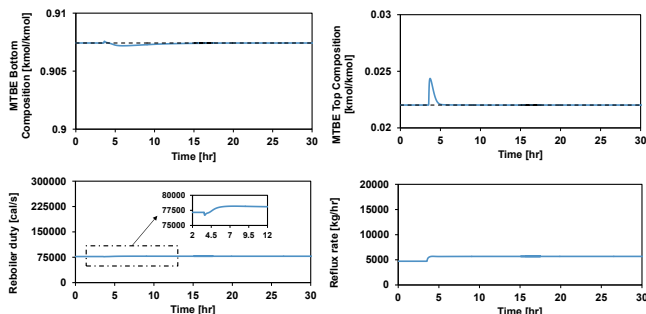


Fig. 6. Closed-loop performance of the optimal reactive distillation column design

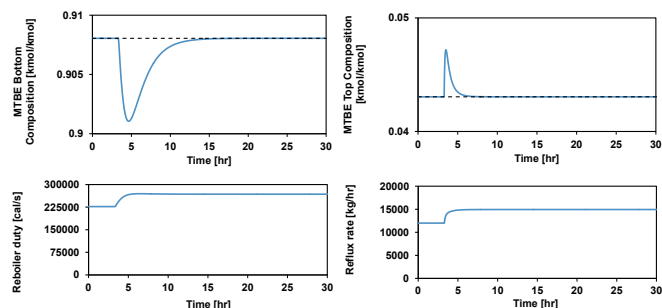


Fig. 7. Closed-loop performance of the design alternative not at the maximum driving force

As it can be noted from Table 4, the RDC design at the maximum driving force has the best controllability performance since the values of IAE and TV in both top and bottom control loops is minimum. Also, the optimal design has the least value of the objective function.

Table 4. Performance metrics for the optimal and alternative designs

Metric	Optimal design	Alternative design
TV – Bottom loop	2154.7	44309
TV – Top loop	1026.22	2947.1
IAE – Bottom loop	1.47E-03	2.49E-02
IAE – Top loop	1.54E-03	3.59E-03
Controller Cost (\$)	107.74	2215.45
f_{obj}	0.851	3.610

4. CONCLUSIONS

In this work, an integrated process design and control of multi-element RDC system was presented. It was verified through steady-state and dynamic analysis that designing RDC at the maximum driving force results in least energy consumption and carbon footprint as well as the best controllability and disturbance rejection. It was also demonstrated that using the equivalent binary element concept is advantageous in designing multi-component reaction-separation operations.

REFERENCES

- Bek-Pedersen, E., Gani, R. (2004). Design and synthesis of distillation systems using a driving-force-based approach, *Chem. Eng. Process.*, 43, 251–262.
- Hamid, M.K.A., Sin, G., and Gani, R. (2010). Integration of process design and controller design for chemical processes using model-based methodology. *Comput. Chem. Eng.*, 34, 683–699.
- Hengstebeck, R.J. (1961). In: Kister, H.Z. (Ed.), *Distillation Design*. McGraw-Hill, Inc., New York, USA, 64–71.
- Jantharasuk, A., Gani, R., Górák, A., Assabumrungrat, S. (2011). Methodology for design and analysis of reactive distillation involving multielement systems. *Chem. Eng. Res. Des.*, 89, 1295–1307.
- Kalukul, S., Malakul, P., Siemanond, K., Gani, R. (2014). Integration of life cycle assessment software with tools for economic and sustainability analyses and process simulation for sustainable process design. *J. Clean Prod.*, 71, 98–109.
- Mansouri, S.S., Sales-Cruz, M., Huusom, J.K., Woodley, J.M., Gani, R. (2015). Integrated process design and control of reactive distillation processes. *IFAC PapersOnLine*, 48 (8), 1120–1125. doi: 10.1016/j.ifacol.2015.09.118
- Mansouri, S.S., Ismail, M.I., Babi, D.K., Simasatitkul, L., Huusom, J.K., Gani, R. (2013). Systematic sustainable process design and analysis of biodiesel processes. *Processes* 1 (2), 167–202. doi: 10.3390/pr1020167
- Michelsen, M.L. (1989). Calculation of multiphase ideal solution chemical equilibrium, *Fluid Phase Equilib.*, 53, 73–80.
- Pérez-Cisneros, E.S. (1997). *Modelling, design and analysis of reactive separation processes*, Ph.D. Thesis, Technical University of Denmark, Lyngby, Denmark.
- Russel, B. M., Henriksen, J. P., Jørgensen, S. B., Gani, R. (2002). Integration of design and control through model analysis. *Comput. Chem. Eng.*, 26, 213–225.
- Ricardez-Sandoval, L.A., Budman, H.M., Douglas, P.L. (2009). Integration of design and control for chemical processes: A review of the literature and some recent results. *Annu. Rev. Control*, 33, 158–171.
- Rivera, D.E., Morari, M., Skogestad, S. (1986). Internal model control: PID controller design. *Ind. Eng. Chem. Process Des. Dev.*, 25, 252–265.